Journal of Translational Medicine

RESEARCH

Open Access

Accumulated β-catenin is associated with human atrial fibrosis and atrial fibrillation

Ying Bai[1], Rui Li[2], Jun-Feng Hao[3], Lian-Wan Chen[4], Si-Tong Liu[1], Xi-Lin Zhang[1], Gregory Y. H. Lip[5,6], Jin-Kui Yang[7], Yi-Xi Zou[8*] and Hao Wang[9*]

Abstract

Background Atrial fibrillation (AF) is associated with increased risk of stroke and mortality. It has been reported that the process of atrial fibrosis was regulated by β-catenin in rats with AF. However, pathophysiological mechanisms of this process in human with AF remain unclear. This study aims to investigate the possible mechanisms of β-catenin in participating in the atrial fibrosis using human right atrial appendage (hRAA) tissues .

Methods We compared the difference of β-catenin expression in hRAA tissues between the patients with AF and sinus rhythm (SR). The possible function of β-catenin in the development of AF was also explored in mice and primary cells.

Results Firstly, the space between the membrane of the gap junctions of cardiomyocytes was wider in the AF group. Secondly, the expression of the gap junction function related proteins, Connexin40 and Connexin43, was decreased, while the expression of β-catenin and its binding partner E-cadherin was increased in hRAA and cardiomyocytes of the AF group. Thirdly, β-catenin colocalized with E-cadherin on the plasma membrane of cardiomyocytes in the SR group, while they were dissociated and accumulated intracellularly in the AF group. Furthermore, the expression of glycogen synthase kinase 3β (GSK-3β) and Adenomatous Polyposis Coli (APC), which participated in the degradation of β-catenin, was decreased in hRAA tissues and cardiomyocytes of the AF group. Finally, the development of atrial fibrosis and AF were proved to be prevented after inhibiting β-catenin expression in the AF model mice.

Conclusions Based on human atrial pathological and molecular analyses, our findings provided evidence that β-catenin was associated with atrial fibrosis and AF progression.

Keywords Atrial fibrillation, Human right atrial appendage, B-catenin, Atrial fibrosis

*Correspondence:
Yi-Xi Zou
xihun00@sina.com
Hao Wang
hwang@mail.ccmu.edu.cn
[1]Cardiovascular Center, Beijing Tongren Hospital, Capital Medical University, Beijing 100730, China
[2]Department of Pathology, Beijing Tongren Hospital, Capital Medical University, Beijing, China
[3]Core Facility for Protein Research, Institute of Biophysics, Chinese Academy of Sciences, Beijing 100101, China
[4]National Laboratory of Biomacromolecules, CAS Center for Excellence in Biomacromolecules, Institute of Biophysics, Chinese Academy of Sciences, Beijing 100101, China
[5]Liverpool Centre for Cardiovascular Science at University of Liverpool, Liverpool John Moores University and Liverpool Heart & Chest Hospital, Liverpool, UK
[6]Danish Center for Health Services Research, Department of Clinical Medicine, Aalborg University, Aalborg, Denmark
[7]Department of Endocrinology, Beijing Key Laboratory of Diabetes Research and Care, Beijing Diabetes Institute, Beijing Tongren Hospital, Capital Medical University, Beijing 100730, China
[8]Department of Cardiac Surgery, Beijing Anzhen Hospital, Capital Medical University, Beijing 100029, China
[9]Beijing Key Laboratory of Diabetes Research and Care, Beijing Diabetes Institute, Beijing Tongren Hospital, Capital Medical University, Beijing 100730, China

Introduction

Atrial fibrillation (AF) is the most common sustained arrhythmia, leading to increased risk of stroke, heart failure and dementia, as well as hospitalizations [1]. Despite the use of oral anticoagulation, there is still high residual risk of stroke, requiring an integrated care approach to its evaluation [2, 3] and management. [4] Though atrial fibrosis is believed to contribute greatly to the development of AF, the exact pathophysiological mechanisms remain unclear.

Previous studies have shown that β-catenin is activated during wound healing [5], myocardial infarction [6], and pulmonary fibrosis [7]. The accumulation of β-catenin in hearts is associated with severe epicardial fibrosis [8]. In addition, the translocation of β-catenin is involved in epithelial- mesenchymal transition, which is an initial and critical step in the processes of fibrosis, such as myocardial infarction repair [6, 7]. Since β-catenin could modulate the intercellular junction of the cardiomyocytes [9] and participate in the atrial fibrosis of AF in the rats [10], the possible role of β-catenin in the initiation of atrial fibrosis and the development of AF in human merits further exploration.

Intercalated disc includes zonula adherents, desmosome and gap junction. The former two types are named as anchoring junctions, which are mainly composed of Cadherins. Gap junctions are connection channels made up of a family of transmembrane proteins called connexins (Cx), which allow the transfers of ions, small molecules and electrical communions between adjacent cardiomyocytes [11]. Cx40 and Cx43 are the main constituents of atrial myocyte closely related with atrial fibrosis and AF [12, 13]. β-catenin participates in the co-localization as part of the gap junction plaque complex by interacting with the carboxyl terminal domain of Cx43 directly [14]. β-catenin also plays important roles in the adherence between atrial cells by binding to E-cadherin cytoplasmic domains directly [15–17]. To maintain a proper adherent role during cardiac development, β-catenin is mainly degraded by a destruction complex after translocation into the cytoplasm, which consists of Adenomatous Polyposis Coli (APC), Axin and various kinases, such as glycogen synthase kinase 3β (GSK-3β) [18, 19]. APC is identified as a tumor suppressor gene, which could regulate cytoplasmic levels of β-catenin by participating in β-catenin degradation in the proteasome [20].

This study aimed to investigate the possible proteins and pathways participating in the AF development using atrial tissues of 32 AF and 35 sinus rhythm (SR) patients with the method of pathological analysis, molecular analysis, immunofluorescence and electron microscopy. The possible mechanisms of β-catenin participating in the AF development were further explored in the mice model of AF and then confirmed in the atrial myocytes of the mice.

Methods

The study was conducted in accordance with the Declaration of Helsinki (as revised in 2013). The study was approved by clinical research ethics committee of Beijing Tongren Hospital (No.2021-041) and Beijing Anzhen Hospital (No. 2021038X), Capital Medical University and individual written consent was obtained from each patient before inclusion. Animal experiments followed the national ethical guidelines implemented by our Institutional Animal Care and Use Committee and were approved by the Ethical Review Committee of the Institute of Zoology, Capital Medical University, Beijing, China.

Patients with atrial fibrillation and sinus rhythm

In our centers, we collected human right atrial appendage (hRAA) samples from 67 patients undergoing cardiac surgery, including cardiac bypass grafting, valvular replacement, modified Morrow procedure and aortic replacement. Inclusion criteria were age older than 18 years old. Intraoperative samples were taken out before radiofrequency ablation or maze operation in order to reduce the impact caused by these procedures. To maintain consistency among the patients, those with histories of cardiac surgery, atrial radiofrequency ablation or cryoablation were excluded. Patients with post-operative AF were also excluded from the study. Included patients were divided into AF group and SR group according to whether they had prior AF based on their medical history and again through electrocardiogram (ECG) or Holter during their hospital stay.

Animals

12-week male C57Bl/6 mice with a body weight range of 22 g to 26 g were housed in a circumstance with food and water ad-libitum and every 12 h of light-dark cycle. The mice were fed with normal diet chow (ND) or high fat diet chow (HFD) (60% fat, 20% carbohydrate, and 20% protein in calorie percentage; Research DIETS, D12492, New Brunswick, NJ, USA) for 8 weeks, respectively. Pyrvinium pamoate (PYP) was injected intraperitoneally at the dose of 2 μg/g body weight to inhibit β-catenin. HFD induced mice were then randomly separated into two groups (vehicle Group and PYP Group) and were administrated with 5-day consecutive intraperitoneal injection of 0.5% CMCNa (vehicle) or PYP, respectively. All animal experiments were performed in accordance with the rules and regulations of the Animal Care and Experimentation Committee, Capital Medical University.

Separation of cardiomyocytes

Primary atrial myocytes were separated from adult mice and hRAA with the method described elsewhere [21, 22]. Briefly, atrial tissue was separated and gently minced to 1 mm^3 pieces in cold Hank's Balanced Salt Solution (HBSS) without Ca^{2+} and Mg^{2+} and mechanically digested with 0.125% type II collagenase (17101015, Gibco) and 0.05% Trypsin (Gibco) buffer at 37 °C. The supernatant was discarded once it became obscure and the pellets were digested with the same buffer without trypsin at 37 °C again. Then the supernatant was collected and centrifuged at 100×g for 2 min. The pellet was resuspended with HBSS and filtered with a 100 μm filter. After centrifugation, the pellet was resuspended with culture medium and plated in a cell culture flask for 1 h to separate the fibroblasts and cardiomyocytes. The supernatants containing cardiomyocytes were plated in a new cell culture flask and maintained in a humidified incubator with 5% CO_2 at 37 °C. The cardiomyocytes were cultured in Dulbecco's Modified Eagle's Medium /Nutrient Mixture F-12 (DMEM/F12, Gibco) with 10% fetal bovine serum (FBS, Gibco), 1% penicillin-streptomycin (Beyotime). 100 μM bromodeoxyuridine (BrdU) were added to inhibit proliferation of fibroblasts. The cardiomyocytes were collected for further analysis after 24 h of culture.

Electrophysiology and stimulation

The stimulation process was described previously [23]. In the anesthetized mice, subcutaneous needle electrodes were placed in the limbs for recordings of lead II electrocardiography. After catheter was tunneled into the esophageal, PowerLab system (AD Instruments, Australia) was used to record esophageal electrocardiogram and monitor the electrical signals by connecting to the first two pairs of electrodes in the catheter. A wave and V wave were corresponded to the P wave and QRS wave in the surface ECG, respectively. The catheter was advanced toward the right atrium until both electrode pairs were correctly placed at the back of the right atrium. And then atrial stimulation was performed to induce AF by switching the first pair of electrodes to connect the stimulator. The stimuli of bidirectional pulses was used with high pass at 50 Hz, duration at 1 ms and amplitude at 10 V, lasting for 15s.

Histopathology and immunohistochemistry staining

For histological analysis, the hRAA tissues were fixed in 4% (v/v) paraformaldehyde solution and the paraffin sections (3 μm) were prepared routinely [24, 25]. Hematoxylin and eosin (HE) staining was used to identify histopathological changes in the hRAA. Masson's trichrome staining was performed to determine the degree of collagen fiber [26]. The area percentage of fiber was further quantitatively analyzed using Halo v3.3 Area Quantification. The previously described method was used for immunohistochemical analysis [24]. The deparaffinized tissue Sect. (3 μm) underwent antigen retrieval with EDTA (pH9.0) and then were incubated with 0.3% H_2O_2 in methanol to inactivate the endogenous peroxidase. The samples were incubated overnight at 4 °C with primary antibodies as follows: β-catenin (ZM-0442, UMAB15, ZSGB-Bio, Beijing, China), E-cadherin (ZA-0565, EP6, ZSGB-Bio, Beijing, China), APC (ZA-0012, ZSGB-Bio, Beijing, China), GSK-3β (22104-1-AP, Proteintech, Wuhan, China), Connexin 40 (sc-365107, Santa Cruz, Dallas, USA) and Connexin43 (26980-1-AP, Proteintech, Wuhan, China) and Wnt1 (GB11822, Servicebio, Wuhan, China). After washing in phosphate-buffered saline (PBS), sections were incubated with biotinylated goat anti-mouse or goat anti-rabbit IgG (ZSGB-Bio, Beijing, China) for 1 h at room temperature. For visualization of the immunoreactive sites, sections were incubated in 0.025% 3,3-diaminobenzidine and 0.01% hydrogen peroxide for 3 min and the nuclear was counterstained with hematoxylin. PBS was used for dilution and washing during the whole protocol. All images were captured using 3D scanner. The positive signals of immunohistochemistry were quantitatively analyzed with Halo3.3 Multiplex IHC.

Western blotting

Western blot experiments were performed as previously described [27]. Proteins were extracted from hRAA tissues, isolated hRAA cardiomyocyte, mice atrial tissues or mice atrial cardiomyocytes using a radioimmunoprecipitation assay (RIPA) (Beyotime, Shanghai, China) lysis buffer with 1 mM phenylmethylsulfonyl fluoride (PMSF) and complete protease inhibitor cocktail (Roche, Switzerland). After clearing the lysates by centrifugation at 15,000 rpm for 15 min at 4 °C, the supernatants were subjected to sodium dodecyl-sulfate polyacrylamide gel electrophoresis (SDS-PAGE) and then transferred to a polyvinylidene difluoride (PVDF) membrane. The PVDF membrane was blocked with Tris Buffered Saline (TBS) with Tween (TBST, TBS plus 0.1% Tween-20) containing 0.5% nonfat dried milk powder, and then were incubated with primary antibodies including rabbit anti-Connexin43 (26980-1-AP, Proteintech, Wuhan, China), mouse anti-E-cadherin (60335-1-Ig, Proteintech, Wuhan, China), rabbit anti-GSK-3β (22104-1-AP, Proteintech, Wuhan, China), rabbit anti-α-actin (23660-1-AP, Proteintech, Wuhan, China), mouse anti-Connexin40 (sc-365107, Santa Cruz, Dallas, USA), mouse anti-Wnt1 (sc-514531, Santa Cruz, Dallas, USA), mouse anti-APC (sc-9998, Santa Cruz, Dallas, USA), rabbit anti-β-catenin (ab32572, Abcam, Cambridge, UK), rabbit anti-Phospho-β-catenin (Ser33/37/Thr41) (9561, Cell Signaling Technology, Massachusetts, USA), rabbit

anti-Phospho-GSK-3β (Ser9) (5558, Cell Signaling Technology, Massachusetts, USA) and mouse anti-GAPDH (M171, MBL, Tokyo, Japan) overnight at 4 °C. After that, incubation was proceeded with secondary antibodies including HRP-conjugated goat anti-rabbit IgG and HRP-conjugated goat anti-mouse IgG antibodies (1:2000, Beyotime, China) for 1 h at room temperature. It was then washed five times with TBST. The immunoreactive bands were detected using enhanced chemiluminescence (Amersham Biosciences, USA) and a LAS-500 chemiluminescence detection system (GE Healthcare Bioscience, USA). Optical density values of immunoreactive bands were obtained using Image J software.

Immunofluorescence

Immunofluorescence experiments were performed as previously described [28]. Human RAA frozen Sect. (5 μm thickness) were fixed with 3% paraformaldehyde in PBS for 30 min and permeabilized with 0.1% Triton X-100 in PBS for 30 min, then blocked with PBS containing 1% bovine serum albumin (BSA) for 30 min. The coverslips were incubated overnight at 4 °C with primary antibodies (diluted at 1:100) as follows: mouse anti-E-cadherin, rabbit anti-β-catenin, rabbit anti-Connexin43 and a mouse anti-Connexin40. The samples were washed three times with PBS, and then were subsequently incubated with goat anti-mouse Alexa Fluor 488, goat anti-mouse Alexa Fluor 488 and goat anti-rabbit Alexa Fluor 568 secondary antibodies (Invitrogen; diluted at 1:500) for 60 min. After being washed five times with PBS, the samples were mounted using mounting solution contained 4′,6-diamidino-2-phenylindole (DAPI, for nuclear staining) reagent (Beyotime, Shanghai, China). Confocal imaging was performed using a FV-3000 (Nikon) confocal laser scanning microscope equipped with a 100× oil immersion objective lens (1.49 NA) and FV31S-SW. The images were adjusted using FV31S-SW and Image J software. Pearson correlation coefficient (PCC) was used to quantify the degree of colocalization between fluorophores [29].

Table 1 The baseline characteristics of the included patients

	SR	AF	P value
No. of patients	35	32	NA
Age	56.71 ± 15.03	59.56 ± 11.73	0.08
Male	17(48.57)	17(53.12)	0.71
Smoking habit	8(22.86)	10(31.25)	0.44
Drinking habit	8(22.86)	4(12.50)	0.32
Hypertension	13(37.14)	11(34.38)	0.81
DM	5(14.29)	2(6.25)	0.50
Heart Failure	8(22.86)	11(34.38)	0.30
Surgery			
Valvular Replacement	11 (31.43)	21(65.63)	0.01
CABG	6(17.14)	6(18.75)	0.88
Modified Morrow	17(48.57)	3(9.38)	0.001
Aortic replacement	1(2.86)	2(6.25)	0.94
LAD	42.22 ± 8.19	49.21 ± 10.09	0.004
LVEF	62.44 ± 9.66	56.45 ± 7.63	0.008

No., Number; NA, not available; AF, Atrial fibrillation; SR, Sinus Rhythm; DM, diabetes mellitus; CABG, coronary artery bridging graft; LAD, left atrial diameter; LVEF, left ventricle ejection fraction

Transmission electron microscopy

The hRAA tissues from surgery were put immediately into cold phosphate buffer containing 2.5% glutaraldehyde and cut into 1 mm^3. After 2 h at room temperature, they were moved to 4℃. After 1 h rinse in water, the samples were post-fixed with 1% OsO_4 for 2 h on ice. Then they were washed in water and stained with 1% uranyl acetate at 4℃ overnight. Later the samples were rinsed, dehydrated in graded alcohols, and embedded in Embed 812 resin. After 48 h curing at 60 °C, ultrathin sections (70 nm) were cut on a Leica UC6 ultramicrotome and collected on formvar-coated copper grids. Images were captured by a FEI Tecnai Sprit 120 kV transmission electron microscope operated at 100 kV. The distance between gap junctions was calculated with Image J software and were quantified by averaging multiple areas from each studied tissue.

Statistical analysis

All quantitative data were expressed as mean ± standard error (SE) and calculated using the Student *t* test. The P values < 0.05 were considered as significant difference. All the statistical analyses were performed by SPSS 21.0 (IBM, Chicago, USA).

Results

Baseline characteristics

Of the 67 included patients, 35 had SR and 32 had AF. All the AF cases were found before the surgery and their median duration of AF was 1.0 year (interquartile range [IQR]: 0.25, 4.00). The duration of each patient's AF was listed in Table S1. Of the AF patients, 18 already had oral anticoagulant treatment before their admission to the hospital and the other 14 had oral anticoagulant treatment initiated during their hospital stay. As shown in Table 1, the included patients were mainly complicated with valvular disease, obstructive hypertrophic cardiomyopathy (HCM), coronary heart disease and aortic disease. Some patients had increased atrial afterload caused by valvular disease and HCM.

Atrial cardiomyocytes become hypertrophic and replaced by fibrosis in AF

To study the pathological changes, we performed histologic analysis of hRAA samples from SR and AF patients. HE staining showed atrial myocyte hypertrophy with degenerated or elongated nuclear, consistent with

previous studies exploring the structural changes of atrial tissues in the AF patients [30, 31]. (Fig. 1A and B). Atrial tissue fibrosis was detected by Masson's trichrome staining. We identified that atrial cells were more prone to be replaced by fibrosis in the atrial tissues of AF patients (Fig. 1C, D and E), which indicated changed myocardial structure by interstitial fibrosis and perivascular fibrosis. These findings suggested that cardiomyocytes were impaired and replaced by fibrosis in the AF patients.

Broader distance between membrane of the gap junction related to atrial fibrosis in hRAA of AF

To explore the ultra-structural changes of hRAA, which was possibly related to atrial fibrosis, transmission electronic microscopy was conducted in samples from 5 SR patients and 5 AF patients. As shown in the photographs, the space between the membranes of the gap junctions was broader in the AF group compared to the SR group (Fig. 2A and B). Analysis further confirmed the distance between the membrane of the gap junction was broader in hRAA of the AF patients (Fig. 2C). These results provided evidence that impaired gap junctional coupling between cardiomyocytes might participate in the progression of myocardial disease.

Contribution of reduced expression of connexin40 and connexin43 to impaired gap junction in hRAA of AF

Since Cx40 and Cx43 were the principal constituents of the multiple gap junction proteins, their protein expression levels were checked in hRAA tissues from SR and AF patients with western blot analysis to further confirm the impairment of the gap junctions [32, 33]. As we speculated, both the protein expression levels of Cx40 (Fig. 3A and B) and Cx43 (Fig. 3H and I) were significantly decreased in the AF group compared to those of the SR group. We further confirmed the decrease expression of Cx40 and Cx43 of the AF group in the cardiomyocytes

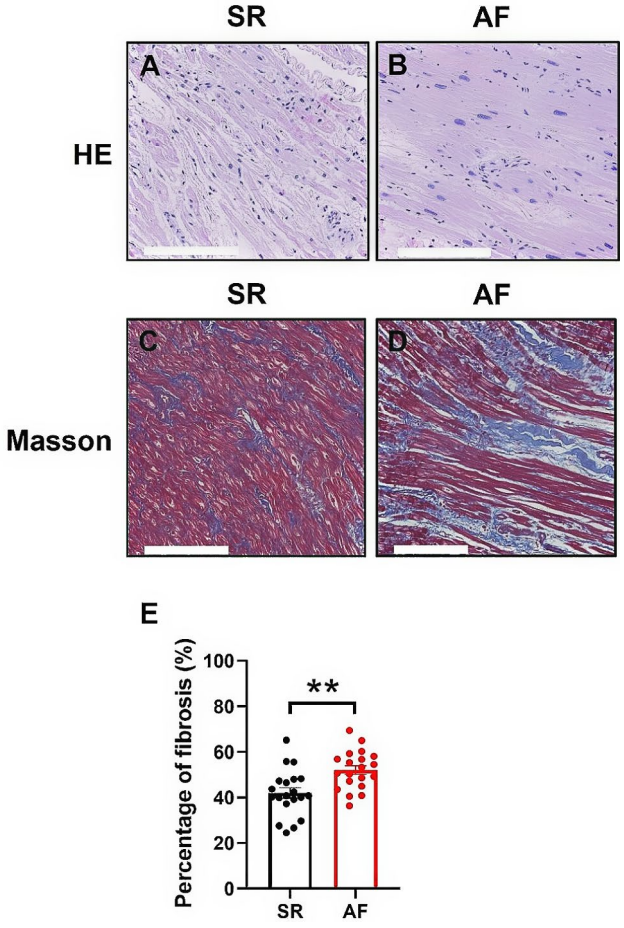

Fig. 1 Increased fibrosis in the hRAA of AF patients. (**A**, **B**) Representative figures of the Hematoxylin-eosin staining of hRAA tissues from 20 SR (**A**) and 20 AF (**B**) patients. Bar: 200 μm. (**C**, **D**) Masson's trichrome staining of hRAA tissues from 20 SR (**C**) and 20 AF (**D**) patients. Bar: 200 μm. (**E**) Percentage of fibrosis area was calculated from Masson's trichrome staining ($n=20$ for each group). The statistical significance of differences between means was assessed by Student *t* test. $^{**}p<0.01$. SR: sinus rhythm; AF: atrial fibrillation; hRAA, human right atrial appendage

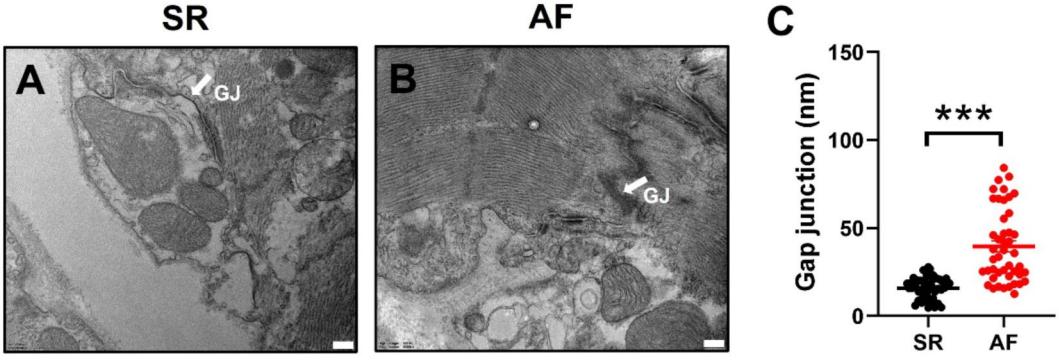

Fig. 2 Impaired gap junction in the hRAA of AF patients. Transmission electron microscopic analysis of human RAA tissues from 5 SR and 5 AF patients. (**A**,**B**) Electron microscopic graphs showed ultrastructural structure of human RAA sections from SR and AF patients. White arrows indicated gap junctions (GJ). Bar, 200 nm. (**C**) Analysis of distance of gap junction ($n=45$ for SR from 5 SR patients, $n=45$ for AF from 5 AF patients). The statistical significance of differences between means was assessed by Student *t* test. $^{***}p<0.001$. SR: sinus rhythm; AF: atrial fibrillation; RAA, right atrial appendage

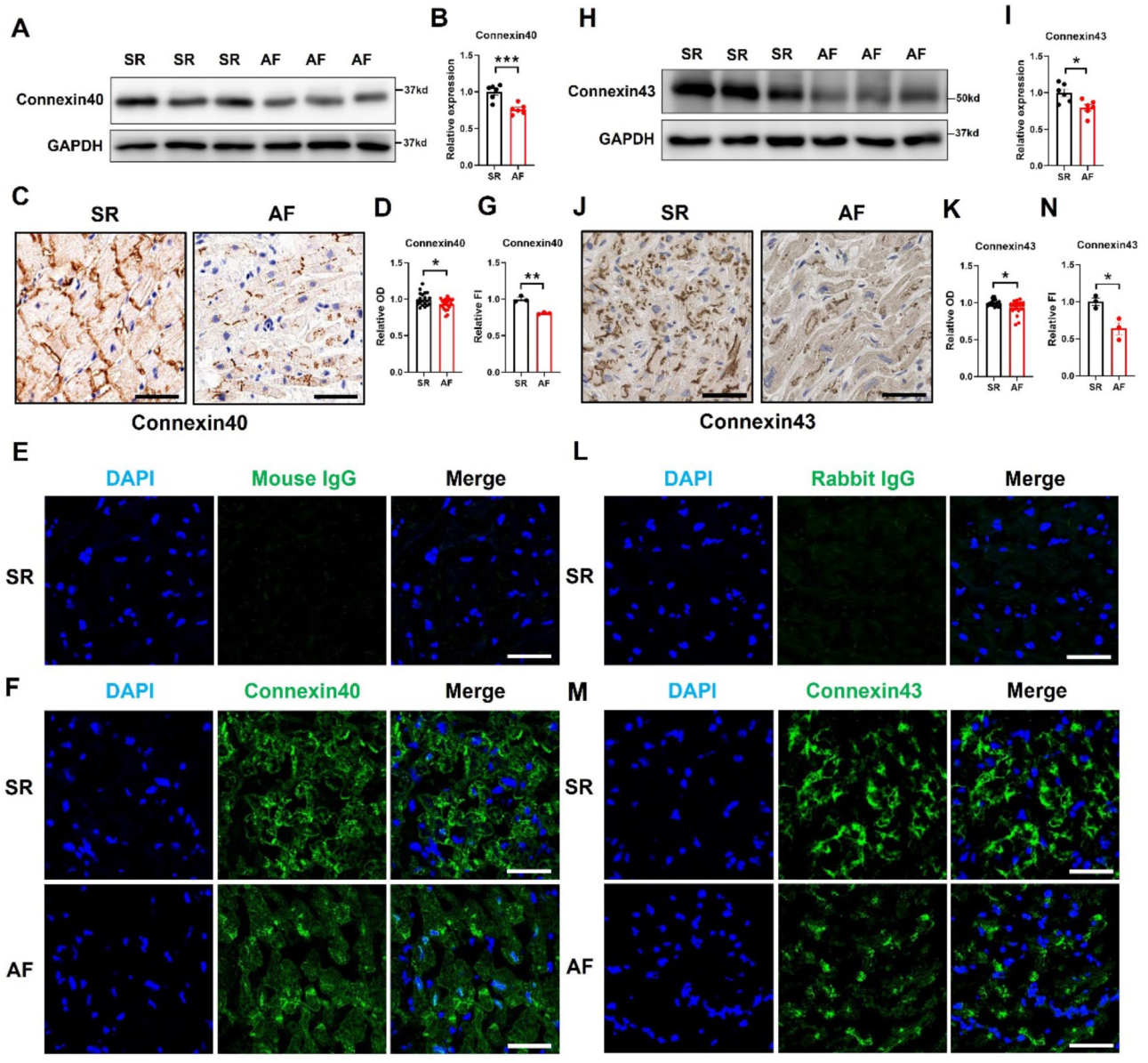

Fig. 3 Decreased expression of Connexin 40 and Connexin 43 in the hRAA of AF patients. (**A**, **H**) Western blot analysis of protein expression level of Connexin 40 (**A**) and Connexin 43 (**H**) in human RAA tissues from SR and AF patients. (**C**, **J**) Immunohistochemistry analysis of Connexin 40 (**C**) and Connexin 43 (**J**) in human RAA tissues from SR and AF patients. Bar, 50 μm. (**B**, **I**) Expression level of Connexin 40 (**B**) and Connexin 43 (**I**) proteins from western blot analysis were quantified by densitometric analyses ($n=6$ for each group). (**D**, **K**) Positive cytoplasm OD of Connexin 40 (**D**) and Connexin 43 (**K**) from immunohistochemistry analysis were calculated from cytoplasm positive signal ($n=20$ for each group). Mouse IgG (**E**) and Rabbit IgG (**L**) were used as negative controls for Cx40 and Cx43 immunostaining respectively. (**F**, **M**) Immunofluorescence analysis of localization of Connexin 40 (green) (**F**) and Connexin 43 (green) (**M**) in human RAA sections from SR and AF patients. Bar, 50 μm. Nuclei (blue) were stained with DAPI. (**G**, **N**) Relative fluorescence-intensity of F and M respectively ($n=3$ for each group). The statistical significance of differences between means was assessed by Student *t* test. *$p<0.05$, **$p<0.01$, ***$p<0.001$. OD, optical density; FI, fluorescence intensity; SR: sinus rhythm; AF: atrial fibrillation; RAA, right atrial appendage

of the hRAA using western blot analysis (Figure S1A-C). To detect the distribution of Cx40 and Cx43, we first performed immunohistochemical staining using hRAA tissue sections. Cx40 (Fig. 3C) and Cx43 (Fig. 3J) mainly expressed on the intercalated discs of the cardiomyocytes in the SR group, but their expression reduced and the distribution became loose in the AF group. The total amount of Cx40 and Cx43 immunoreactive signals of immunohistochemical staining were reduced in the AF group (Fig. 3D, K), consistent with western blot data analysis. Then we performed an immunofluorescence analysis in the hRAA tissue frozen sections for further confirmation. Mouse IgG (Fig. 3E) and rabbit IgG (Fig. 3L) were used as negative controls to verify the specificity of the antibodies

and exclude nonspecific signals. In the SR group, sections stained with the Cx40 (Fig. 3F) or Cx43 (Fig. 3M) antibodies mainly exhibited strong punctate patterns at the intercalated discs between cardiomyocytes. However, AF induced changes in the pattern of distribution of Cx40 (Fig. 3F) and Cx43 (Fig. 3M) respectively. Immunofluorescence intensity of Cx40 (Fig. 3G) and Cx43 (Fig. 3N) were both reduced in AF group than that of SR group. These findings indicated that Cx40 and Cx43 mainly located at the intercalated discs of the cardiomyocytes in SR and their protein expression levels decreased in AF.

Dissociation of β-catenin from E-cadherin and its accumulation in cytosol in hRAA of AF

Previous studies showed that β-catenin possibly participated in the regulation of gap junction between cardiomyocytes [34]. Therefore, to identify the molecular mechanism regulating impaired gap junction and promoting fibrosis progression in AF, we initially checked the expression of β-catenin in the hRAA tissues in addition to cardiomyocytes. Western blot analysis showed protein expression level of β-catenin was remarkably increased in the AF group compared to the SR group both in the hRAA tissues (Fig. 4A, B) and the hRAA cardiomyocytes (Figure S2A and 2 C). β-catenin metabolism is mainly controlled by ubiquitination and proteasomal degradation [35, 36], and the phosphorylation modification of β-catenin is a prerequisite for ubiquitination degradation [37]. So we analyzed the expression of phosphorylation-β-catenin (S33/37/T41) and found a significant reduction in the AF group compared to the SR group both in the hRAA tissues (Fig. 4A, C) or the hRAA cardiomyocytes (Figure S2A and 2D), which induced accumulation of β-catenin in impaired cardiomyocytes from AF patients. To investigate the distributions of β-catenin in the cardiomyocytes, we performed immunohistochemical analysis of hRAA tissue sections from patients with SR and AF. We found that β-catenin mainly located on the cell membrane in the hRAA tissues of SR group (Fig. 4D), but transferred to the cytoplasm of the AF group (Fig. 4D). The total amount of β-catenin immunoreactive signals of immunohistochemical staining was increased in the AF group (Fig. 4E), consistent with western blot data analysis. Because β-catenin usually binds to E-cadherin (a key components of gap junctions) to refrain from degradation [38], we further checked expression of E-cadherin protein and also found it significantly higher in AF group compared to SR group both in the hRAA tissues (Fig. 4F, G) and the hRAA cardiomyocytes (Figure S2A-B). To investigate the distribution of E-cadherin in the cardiomyocytes, we performed an immunohistochemical analysis of hRAA tissue sections from patients with SR and AF. Similar to β-catenin, E-cadherin was mainly located on the cell membrane of the cardiomyocytes in the hRAA tissues of SR group (Fig. 4H), but in the cytoplasm of the AF group (Fig. 4H). The total amount of E-cadherin immunoreactive signals of immunohistochemical staining was increased in the AF group (Fig. 4I), consistent with western blot data analysis. To further analyze distribution of both β-catenin and E-cadherin, immunofluorescence analysis of hRAA tissue sections from patients with SR and AF was performed. Immunofluorescence intensity of β-catenin and E-cadherin from AF tissues were both higher than that of SR tissues (Fig. 4K, L). In the SR group, β-catenin was co-localized with E-cadherin mainly on the cell membrane (Fig. 4J, M). However, in the AF group, β-catenin was dissociated with E-cadherin and preferentially localized intracellularly (Fig. 4J, M). The colocalization of β-catenin with DAPI was more common in the AF group, indicating that there was more nuclear β-catenin in the AF group (Fig. 4J, N). These findings suggested that in the impaired cardiomyocytes of AF, both β-catenin and E-cadherin dislocated from the membrane into the cytosolic pool. The subcellular localization of β-catenin and E-cadherin changed simultaneously, possibly because β-catenin played the cell-cell adhesive role by binding directly to the cytoplasmic tail of E-cadherin [39]. They lost anchoring in the membrane due to their dissociation and then translocated into cytosolic pool together in AF.

Accumulation of β-catenin due to decreased GSK-3β and APC in hRAA of AF

β-catenin mainly exists in membrane associated pool, cytosolic pool and nuclear pool [40]. Wnt/β-catenin pathway is important for Cx40 and Cx43 expression in cardiomyocytes [32]. As the ligand of Wnt, cytoplasmic β-catenin was regulated by Wnt and the destruction complex without Wnt stimulation for final degradation [41]. APC and GSK3β are two important regulators in the destruction complex [37]. Wnt-1 in Wnt signaling pathway is reported as a specific substance that induces Cx40 and Cx43 expression in cardiomyocytes [32]. Increased expression of Cx40 and Cx43 participated in the formation of functional gap junctions through signaling transduction of β-catenin [42]. To detect the reason of the accumulation of β-catenin, we firstly investigated the possible related proteins of Wnt1, GSK-3β and APC, with immunohistochemical staining of the hRAA tissues from SR and AF patients. The locations of these proteins in the atrial cells from SR and AF patients were consistent (Fig. 5A-C). Although the expression level of Wnt1 was similar between the AF and SR groups (Fig. 5A, D), the expression levels of GSK-3β (Fig. 5B, E) and APC (Fig. 5C, F) significantly reduced in AF group compared to that of the SR group. We further checked the expression of Wnt1, GSK-3β and APC proteins in hRAA tissues. Consistent with the results of immunohistochemistry,

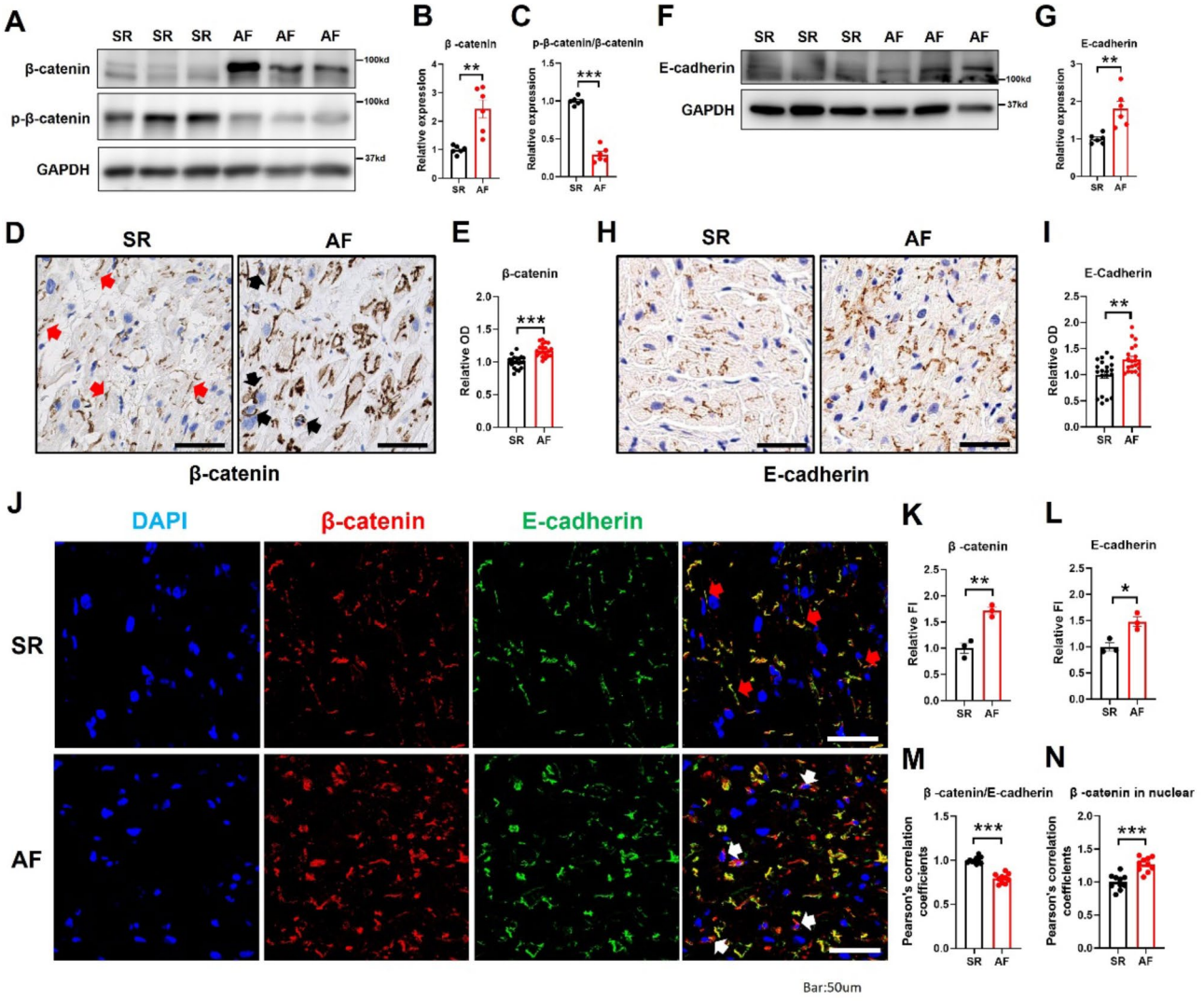

Fig. 4 Increased expression of β-catenin and E-cadherin accompanied with their re-distribution in the hRAA of AF patients. (**A**) Western blot analysis of protein expression level of β-catenin and phosphor-β-catenin in human RAA tissues from SR and AF patients. (**B**, **C**) Expression level of β-catenin (**B**) and ratio of phosphor-β-catenin and β-catenin (**C**) from western blot analysis were quantified by densitometric analyses ($n=6$ for each group). (**D**) Immunohistochemistry analysis of β-catenin in human RAA tissues from SR and AF patients. Red arrows indicated normal location of β-catenin at plasma membrane in human cardiomyocyte from SR patients, whereas black arrows indicated distribution of β-catenin at nucleus in human cardiomyocyte from AF patients. Bar, 50 μm. (**E**) Positive cytoplasm OD of β-catenin from immunohistochemistry analysis were calculated from cytoplasm positive signal ($n=20$ for each group). (**F**) Western blot analysis of protein expression level of E-cadherin in human RAA tissues from SR and AF patients. (**G**) Expression level of E-cadherin from western blot analysis were quantified by densitometric analyses ($n=6$ for each group). (**H**) Immunohistochemistry analysis of E-cadherin in human RAA tissues from SR and AF patients. Bar, 50 μm. (**I**) Positive cytoplasm OD of E-cadherin from immunohistochemistry analysis were calculated from cytoplasm positive signal ($n=20$ for each group). (**J**) Immunofluorescence analysis of localization of E-cadherin (green) and β-catenin (red) in human RAA sections from SR and AF patients. Nuclei (blue) were stained with DAPI ($n=3$ for each group), red arrows indicated normal location of β-catenin and E-cadherin at plasma membrane in human cardiomyocyte from SR patients, whereas white arrows indicated re-distribution of β-catenin at nucleus in human cardiomyocyte from AF patients. Bar, 50 μm. (**K**, **L**) Relative fluorescence-intensity of β-catenin and E-cadherin respectively ($n=3$ for each group). (**M**) Histogram representing colocalization of β-catenin and E-cadherin from SR and AF groups by using Pearson's correlation coefficients analysis. (**N**) Histogram representing colocalization of β-catenin and DAPI from SR and AF groups by using Pearson's correlation coefficients analysis. The statistical significance of differences between means was assessed by Student *t* test. *$p<0.05$, **$p<0.01$, ***$p<0.001$. OD, optical density; FI, fluorescence intensity; SR: sinus rhythm; AF: atrial fibrillation; RAA, right atrial appendage

we found that the expression level of Wnt1 (Fig. 5G, K) was not changed, while the expression levels of GSK-3β (Fig. 5G, H) and APC (Fig. 5G, J) were significantly lower than that of the SR group. GSK-3β is mainly responsible for phosphorylating β-catenin at the S33/S37/T41 sites. When GSK-3β is phosphorylated at the S9 site (p-GSK-3β (S9)), its kinase activity is reduced and therefore could not effectively phosphorylate β-catenin any more. This allows β-catenin to accumulate in the cytoplasm and potentially enter the cell nucleus for the

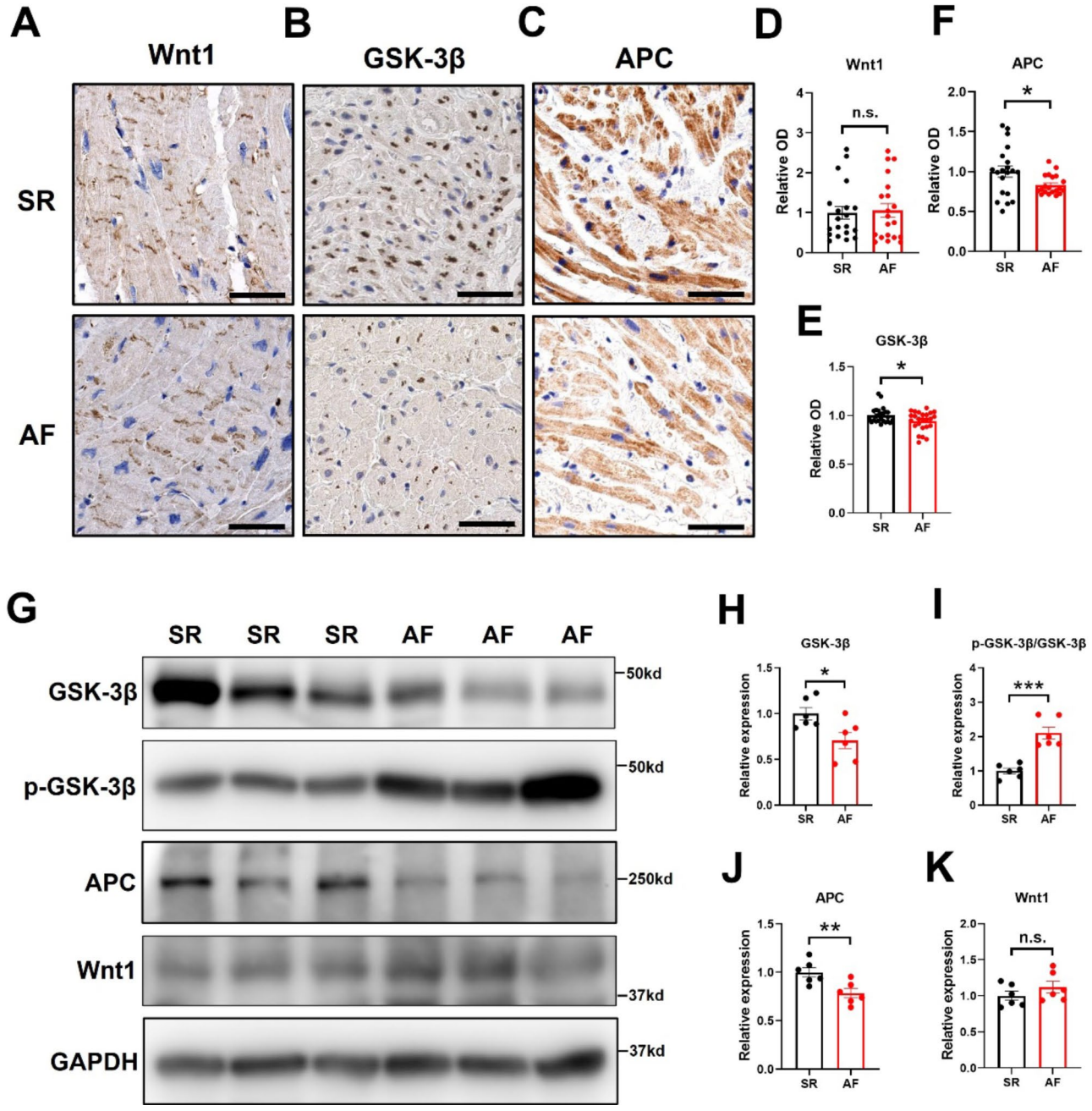

Fig. 5 Decreased expression of GSK-3β and APC in the hRAA of AF patients. (**A-C**) Immunohistochemistry staining of Wnt1(**A**), GSK-3β (**B**) and APC (**C**) from SR and AF human atrial sections. Bar, 50 μm. (**D-F**) Positive cytoplasm OD of Wnt1 (**D**), GSK-3β (**E**) and APC (**F**) were quantified by immunosignal intensity analysis ($n = 20$ from each group for D and F, $n = 25$ from each group for **E**). (**G**) Western blot analysis of Wnt1, GSK-3β, phosphor-GSK-3β and APC in human right atrial tissues from SR and AF patients. (**H-K**) Protein bands of Wnt1, GSK-3β, ratio of phosphor-GSK-3β and GSK-3β and APC from western blot analysis were quantified by densitometric analyses ($n = 6$ for each group). The statistical significance of differences between means was assessed by Student *t* test. *$p<0.05$, **$p<0.01$, ***$p<0.001$, n.s. means not significant. GSK-3β, glycogen synthase kinase 3β; APC, Adenoma Polyposis Coli; OD, optical density; SR: sinus rhythm; AF: atrial fibrillation; RAA, right atrial appendage

regulation of target genes [43]. Our result showed an increase of phosphorylation of GSK-3β in the hRAA tissues of AF (Fig. 5G, I), indicating that the activity of GSK-3β was inhibited in the AF group. In the hRAA cardiomyocytes, similar results to the hRAA tissues could be seen in the AF group (Figure S3A-E). Therefore, the simultaneous reduction of the expression of GSK-3β and APC might play important roles in the accumulation of β-catenin, because they both participated in the degradation of β-catenin.

Inhibition of β-catenin reduce susceptibility to AF in mice

The inhibition of β-catenin in reducing AF susceptibility was derived from human samples with various clinical background in the above study. The obesity-based mice induced with HFD was a clinically common AF induction model built to explore possible mechanisms [44]. ND and HFD mice were given electrical stimulation to induce AF. We showed representative surface and esophageal ECGs of AF and SR as well as the process of AF converting to SR (Fig. 6A). A higher incidence of AF was found in the HFD group (100%) than that in ND group (50%) through electrophysiological analysis (Fig. 6B), which confirmed the effectiveness of the HFD mice as an AF induction model. It has been reported that PYP was a potent inhibitor of β-catenin, which was involved in the inhibition of phosphorylation of GSK3β (S9) via the GSK3β/β-catenin signaling axis [43]. In order to explore the functional roles of β-catenin in the induction and progression of AF, we downregulated the expression of β-catenin in the HFD induced mice models by administration of PYP through 5-day consecutive intraperitoneal injection and then triggered AF with electrical stimulation (Fig. 6C). We isolated cardiomyocytes from the heart and confirmed downregulated expression of β-catenin in the cardiomyocytes after PYP administration by western blot analysis (Fig. 6D, E). ECG results after stimulation showed slightly inhibited frequency of AF episodes by PYP (about 18%) (Fig. 6F) and significantly reduced duration of AF time, because all episodes of AF recovered spontaneously with longer conversion time in the vehicle group than that in the PYP group (Fig. 6G). To explore the signaling pathway of β-catenin in AF development, the expression of the protein in cardiomyocytes from the mice models was checked. In HFD mice, we first confirmed the increase of β-catenin after electrical stimulation, and then the reduction of β-catenin after PYP administration (Fig. 6H, Figure S4A). By contrast, phosphorylation of β-catenin was decreased in the AF model and enhanced after PYP administration to promote the degradation of β-catenin (Fig. 6H, Figure S4B). Cx43 and Cx40 decreased after increasing β-catenin by stimulation, while increased after further inhibiting β-catenin (Fig. 6H, Figure S4F, G). A similar change was seen in E-cadherin to β-catenin with an increase after stimulation and then a decrease after further inhibiting β-catenin (Fig. 6H, Figure S4E). GSK-3β decreased in the HFD mice after stimulation, but had no change after administration of PYP. Phosphorylation of GSK-3β (S9) increased in the AF model, and then decreased after PYP administration (Fig. 6H, Figure S4C, D). Perhaps because APC did not participate in the pathway of inhibiting β-catenin by PYP, APC decreased in HFD mice after the stimulation, but no change was found after further inhibiting β-catenin (Fig. 6H, Figure S4H) [45]. Wnt1 was not changed in the AF model of mice, which was similar to the AF model of human, and it was not changed after further inhibiting β-catenin, as well (Fig. 6H, Figure S4I). Finally, we performed Masson's trichrome staining to analyze the fibrosis of atrial tissues. The results showed severer fibrosis of atrial tissues from the AF model, and it could be alleviated after administration of PYP (Fig. 6I, J). These results indicated a similar change in the AF model of mice to human and the inhibition of β-catenin in mice could also reduce susceptibility to AF in the mice.

Discussion

This study extends our knowledge on the role of β-catenin by exploring the differences of hRAA tissues between AF and SR patients. Accumulation of cytoplasmic β-catenin could be caused by impaired binding ability to E-cadherin on the membrane and decreased GSK-3β and APC in the cytoplasm, in case of high-risk factors of inducing AF (e.g. myocarditis, structural remodeling of atrial and myocardial fibrosis and so on). These could result in decreased expression of Cx40 and Cx43 in the cardiomyocytes, which was associated with the wider space between the membranes of gap junctions in the cardiomyocytes and increased myocardial fibrosis. Furthermore, we confirmed that increased AF susceptibility could be reduced by inhibiting β-catenin accumulation in the cardiomyocytes using PYP.

β-catenin was found as a participating pathway in the regulation of Cx43 in recent studies [9, 46]. We further confirmed their roles in the regulation of gap junction with hRAA tissues and atrial myocytes. Broader distances between the membranes of gap junctions were seen by electron microscopic examinations in the AF group. To investigate the associations between broader gap junctions and AF, possible participating proteins such as Cx40 and Cx43 were further explored, which widely expressed in atrial myocytes and played important roles in atrial remodeling of AF [47–49]. As the main constituent of gap junction that interacted with β-catenin directly, their expression decreased according to the western-blot results. In the immunofluorescence analysis, the expression of Cx40 and Cx43 decreased with loose expression in the AF patients. The electrical signal transduction between atrial myocytes could be disturbed by impaired expression of Cx40 and Cx43 in the atrial tissue, resulting in uneven distribution of electrical signals, reentry or conduction block, and eventually leading to the maintenance or recurrence of AF [50–55]. These results were consistent with previous studies showing that specific knockout of mouse Cx43 can accelerate the formation of fibrosis [49]. In our study, Cx40 decrease could produce similar effect to Cx43 decrease on the progression of fibrosis. One previous study performed on cardiomyocytes through rapidly pacing had similar

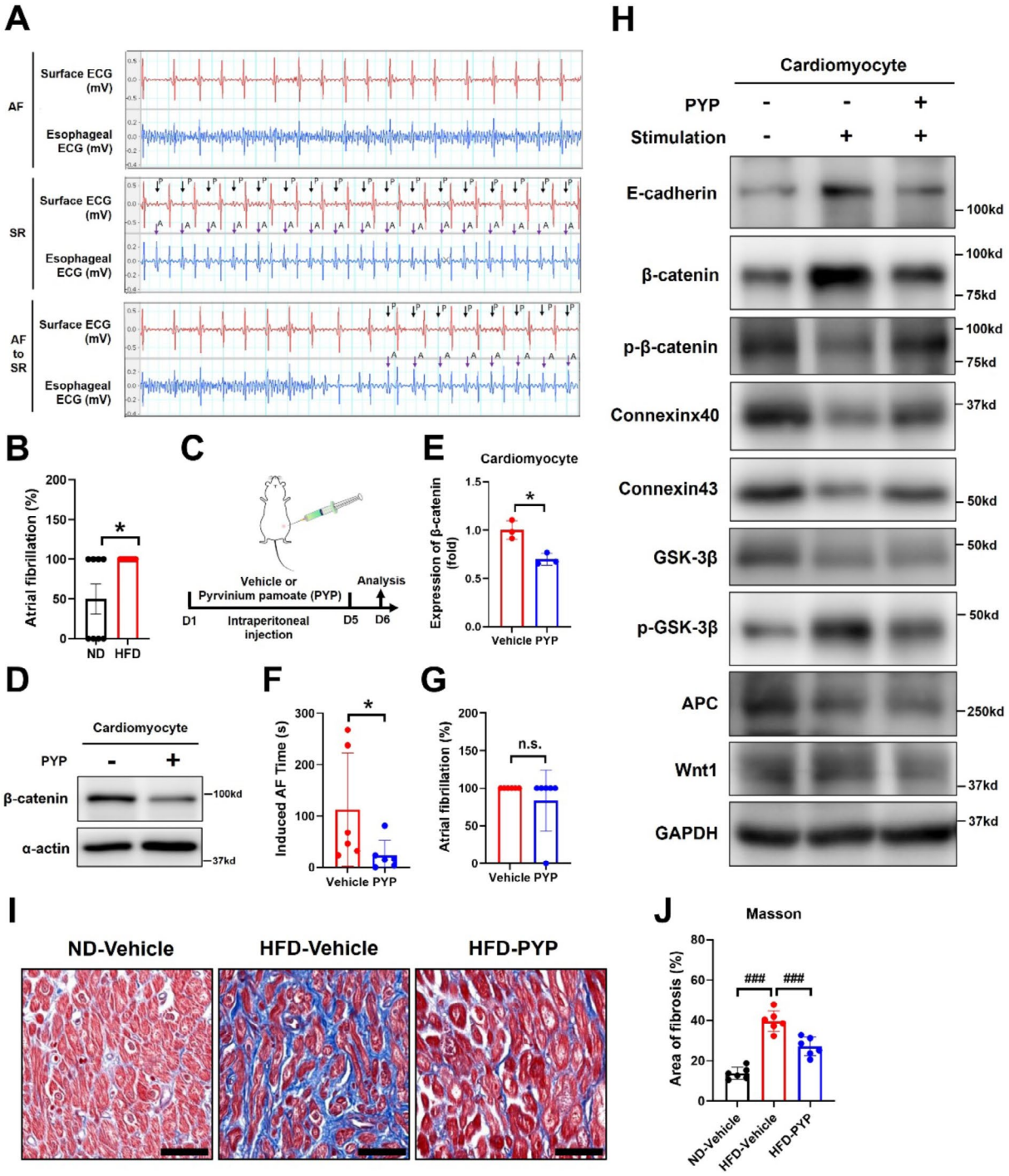

Fig. 6 Relationship of Accumulation of β-catenin to AF Susceptibility. (**A**) Representative surface ECG and esophageal ECG of AF, SR and AF converting to SR in each group. (**B**) Incidence of AF induced by electrophysiologic stimulation in normal diet (ND) and high fat diet (HFD) induced mice ($n=8$ for each group). (**C**) Strategy of analysis of HFD induced mice treated with five-day consecutive intraperitoneal injection of pyrvinium pamoate (2 μg/g body weight). (**D**) Western Blot analysis of β-catenin in cardiomyocyte from pyrvinium pamoate (PYP) treated mice. (**E**) Protein expression level of β-catenin from western blot analysis was quantified by immunosignal intensity analysis ($n=3$ for each group). (**F**) Incidence of AF induced by electrophysiologic stimulation in mice with vehicle or PYP administration. (**G**) Episodes of AF duration before conversion to SR spontaneously in mice with vehicle or PYP administration. ($n=6$ for each group for F and **G**). (**H**) Western Blot analysis of β-catenin signal proteins in cardiomyocyte from vehicle or PYP treated mice with or without electrical stimulation. (*I*) Masson's trichrome staining of heart tissues from 3 groups of ND mice with vehicle administration, HFD mice induced by electrophysiologic stimulation with vehicle or PYP administration. ($n=6$ for each group). Bar, 50 μm. (**J**) Percentage of fibrosis area was analysis from each group. The statistical significance of differences among means was assessed. *$p<0.05$, n.s. means not significant by Student *t* test. $^{###}p<0.001$, n.s. means not significant by one-way ANOVA test. ECG, electrocardiogram; SR: sinus rhythm; AF: atrial fibrillation

results to our study in increasing β-catenin expression, but without impact on the increased Cx43 distribution, which was inconsistent with our results [56]. Then we performed Western-Blot to further explore the relation between β-catenin and Cx expression regulation in the mice models, which showed consistent results with our clinical samples. This mechanism exploration in the mice that Cx43 and Cx40 expression decreased after AF induction, but increased after inhibiting β-catenin further confirmed our results.

Of the several proteins possibly related to the accumulation of cytosolic β-catenin, GSK-3β and APC were found reduced in the AF group, which was different from previously published papers on the roles of β-catenin participating in AF through the pathway of Wnt-β-catenin-LEF1. As a component kinases, GSK-3β played an important role in the regulation of β-catenin expression by participating in its phosphorylation [18, 19]. Therefore, we speculated that the accumulation of β-catenin was caused by its exemption from degradation because the reduction of GSK-3β prevented β-catenin from being phosphorylated [40]. In addition, the disruption of β-catenin in AF patients mainly occurred in its roles of cell adhesion rather than signal transduction [57]. And in this condition, the β-catenin/GSK-3β/APC was not regulated by the Wnt/Wingless signaling pathway, which was consistent with that seen in the hypertrophic cardiomyocyte [57, 58]. However, it is possible that the excessive β-catenin due to reduced cytosolic phosphorylated degradation could be inhibited by Wnt1 [59].

To investigate the functional roles of β-catenin on the AF development, HFD mice were used for building AF models and then PYP was used for the inhibition of β-catenin because of its roles in downregulation of p-GSK-3β (S9) [43]. Based on these findings, we further confirmed the beneficial roles of reducing AF susceptibility by inhibiting β-catenin using mice AF models and then the functional roles of β-catenin through isolating atrial myocyte from the mice hearts. Actually, the structural and distribution change of β-catenin preceding gap junction remodeling was confirmed by one vitro study exploring the impact of rapid electrical stimulation on the alterations in cardiac intercellular junction proteins of cardiomyocytes [9]. And our study further provided evidence that the increase of β-catenin played an important role in gap junction stability, atrial fibrosis and AF progression using hRAA tissues and mice models, respectively. Therefore, we believed the observed changes in β-catenin are specifically causal to the development of AF, not simply the result of a general remodeling process.

In conclusion, we demonstrated that β-catenin accumulation is associated with atrial fibrosis and AF progression through inducing wider space between the membranes of gap junctions. Key factors in this process include (1) dissociation of β-catenin with E-cadherin on the plasma membrane; (2) cytosolic localization of β-catenin and E-cadherin; (3) reduced expression of GSK-3β and APC which were responsible for degradation of β-catenin. Further research will be required to determine the causal relationship between these molecules.

Limitations

First, we only had samples from the right atrial appendage which might be different situations from the left atria appendage or other parts of the atria. Hence, atrial fibrosis and other histological features of structural remodeling in this study mainly derived from analysis of β-catenin on hRAA tissues. Whether the results could be extended to the other parts of the atria needs further verification. Second, the AF was the obesity-induced mice model, which only represented a specific type of AF instead of the general clinical samples of AF. Therefore, the β-catenin signaling mechanism derived from the obesity mice may not be generalized to other AF types.

Supplementary Information

The online version contains supplementary material available at https://doi.org/10.1186/s12967-024-05558-0.

Supplementary Material 1

Acknowledgements

We would like to thank Duo Duo and Qing Bian from Center for Biological Imaging (CBI), Institute of Biophysics, Chinese Academy of Sciences, for technical support with FV3000 confocal imaging and image analysis.

Authors contributions

Ying Bai, Rui Li, Jun-Feng Hao, Lian-Wan Chen, Si-Tong Liu, Xi-Lin Zhang and Hao Wang performed experiments and analyzed data; Ying Bai, Yi-Xi Zou and Hao Wang designed experiments and supported the study; Ying bai and Hao Wang wrote and revised the manuscript; Ying bai, Yi-Xi Zou and Hao Wang supervised the research. Gregory Y. H. Lip and Jin-Kui Yang helped with the interpretation of the results and proofreading of the manuscript.

Funding

This work was supported by National Natural Science Foundation of China (81800291) and the Beijing Municipal Administration of Hospitals Incubating Program (PX2023006) to Ying Bai. It was also supported by National Natural Science Foundation of China (82170809), Beijing Municipal Natural Science Foundation (7232232) and Outstanding Young Talent Program of Beijing Tongren Hospital (2021-YJJ-ZZL-006) to Hao Wang.

Data availability

All of the relevant data and materials are available from the authors upon reasonable request.

Declarations

Ethics approval and consent to participate

The study was approved by clinical research ethics committee of Beijing Tongren Hospital (No.2021-041) and Beijing Anzhen Hospital (No. 2021038X), Capital Medical University and individual written consent was obtained from each patient before inclusion. Animal experiments followed the national ethical guidelines implemented by our Institutional Animal Care and Use Committee and were approved by the Ethical Review Committee of the Institute of Zoology, Capital Medical University, Beijing, China.

Competing interests
The authors declare that they have no conflicts of interest with the contents of this article.

Received: 1 December 2023 / Accepted: 29 July 2024
Published online: 05 August 2024

References

1. Burdett P, Lip GYH. Atrial fibrillation in the Uk: Predicting costs of an emerging epidemic recognizing and forecasting the cost drivers of atrial fibrillation-related costs. Eur Heart J Qual care Clin Outcomes. 2022;8:187–94.
2. Potpara TS, Lip GYH, Blomstrom-Lundqvist C, Boriani G, Van Gelder IC, Heidbuchel H, et al. The 4s-af scheme (stroke risk; symptoms; severity of burden; substrate): a novel approach to in-depth characterization (rather than classification) of atrial fibrillation. Thromb Haemost. 2021;121:270–8.
3. Lip GYH. The abc pathway: an integrated approach to improve af management. Nat Rev Cardiol. 2017;14:627–8.
4. Chao TF, Joung B, Takahashi Y, Lim TW, Choi EK, Chan YH, et al. 2021 focused update consensus guidelines of the asia pacific heart rhythm society on stroke prevention in atrial fibrillation: executive summary. Thromb Haemost. 2022;122:20–47.
5. Cheon SS, Cheah AY, Turley S, Nadesan P, Poon R, Clevers H, et al. Beta-catenin stabilization dysregulates mesenchymal cell proliferation, motility, and invasiveness and causes aggressive fibromatosis and hyperplastic cutaneous wounds. Proc Natl Acad Sci USA. 2002;99:6973–8.
6. Blankesteijn WM, van Gijn ME, Essers-Janssen YP, Daemen MJ, Smits JF. Beta-catenin, an inducer of uncontrolled cell proliferation and migration in malignancies, is localized in the cytoplasm of vascular endothelium during neovascularization after myocardial infarction. Am J Pathol. 2000;157:877–83.
7. Chilosi M, Poletti V, Zamò A, Lestani M, Montagna L, Piccoli P, et al. Aberrant wnt/beta-catenin pathway activation in idiopathic pulmonary fibrosis. Am J Pathol. 2003;162:1495–502.
8. Ye B, Ge Y, Perens G, Hong L, Xu H, Fishbein MC, et al. Canonical wnt/β-catenin signaling in epicardial fibrosis of failed pediatric heart allografts with diastolic dysfunction. Cardiovasc Pathology: Official J Soc Cardiovasc Pathol. 2013;22:54–7.
9. Nakashima T, Ohkusa T, Okamoto Y, Yoshida M, Lee JK, Mizukami Y, et al. Rapid electrical stimulation causes alterations in cardiac intercellular junction proteins of cardiomyocytes. Am J Physiol Heart Circ Physiol. 2014;306:H1324–1333.
10. Lv X, Li J, Hu Y, Wang S, Yang C, Li C, et al. Overexpression of mir-27b-3p targeting wnt3a regulates the signaling pathway of wnt/β-catenin and attenuates atrial fibrosis in rats with atrial fibrillation. Oxidative Med Cell Longev. 2019;2019:1–13.
11. Forbes MS, Sperelakis N. Intercalated discs of mammalian heart: a review of structure and function. Tissue Cell. 1985;17:605–48.
12. Wilhelm M, Kirste W, Kuly S, Amann K, Neuhuber W, Weyand M, et al. Atrial distribution of connexin 40 and 43 in patients with intermittent, persistent, and postoperative atrial fibrillation. Heart Lung Circ. 2006;15:30–7.
13. Wetzel U, Boldt A, Lauschke J, Weigl J, Schirdewahn P, Dorszewski A, et al. Expression of connexins 40 and 43 in human left atrium in atrial fibrillation of different aetiologies. Heart. 2005;91:166–70.
14. Spagnol G, Trease AJ, Zheng L, Gutierrez M, Basu I, Sarmiento C et al. Connexin43 carboxyl-terminal domain directly interacts with β-catenin. Int J Mol Sci. 2018;19.
15. Aberle H, Butz S, Stappert J, Weissig H, Kemler R, Hoschuetzky H. Assembly of the cadherin-catenin complex in vitro with recombinant proteins. J Cell Sci. 1994;107(Pt 12):3655–63.
16. Hülsken J, Behrens J, Birchmeier W. Tumor-suppressor gene products in cell contacts: the cadherin-apc-armadillo connection. Curr Opin Cell Biol. 1994;6:711–6.
17. Jou TS, Stewart DB, Stappert J, Nelson WJ, Marrs JA. Genetic and biochemical dissection of protein linkages in the cadherin-catenin complex. Proc Natl Acad Sci USA. 1995;92:5067–71.
18. Behrens J, von Kries JP, Kühl M, Bruhn L, Wedlich D, Grosschedl R, et al. Functional interaction of beta-catenin with the transcription factor lef-1. Nature. 1996;382:638–42.
19. Antos CL, McKinsey TA, Frey N, Kutschke W, McAnally J, Shelton JM, et al. Activated glycogen synthase-3 beta suppresses cardiac hypertrophy in vivo. Proc Natl Acad Sci USA. 2002;99:907–12.
20. Riedel RF, Agulnik M. Evolving strategies for management of desmoid tumor. Cancer. 2022;128:3027–40.
21. Ackers-Johnson M, Li PY, Holmes AP, O'Brien SM, Pavlovic D, Foo RS. A simplified, langendorff-free method for concomitant isolation of viable cardiac myocytes and nonmyocytes from the adult mouse heart. Circul Res. 2016;119:909–20.
22. Guo G-r, Chen L, Rao M, Chen K, Song J-p. Hu S-s. A modified method for isolation of human cardiomyocytes to model cardiac diseases. J Translational Med. 2018;16.
23. Jiang L, Li L, Ruan Y, Zuo S, Wu X, Zhao Q, et al. Ibrutinib promotes atrial fibrillation by inducing structural remodeling and calcium dysregulation in the atrium. Heart Rhythm. 2019;16:1374–82.
24. Duan M, Hao J, Cui S, Worthley DL, Zhang S, Wang Z, et al. Diverse modes of clonal evolution in hbv-related hepatocellular carcinoma revealed by single-cell genome sequencing. Cell Res. 2018;28:359–73.
25. Bai Y, Shi XB, Zhang YQ, Wang YL, Liu XY, Esteve-Pastor MA. Differences of matrix metalloproteinase 2 expression between left and right ventricles in response to nandrolone decanoate and/or swimming training in mice. Chin Med J (Engl). 2018;131:207–12.
26. Shang L, Pin L, Zhu S, Zhong X, Zhang Y, Shun M, et al. Plantamajoside attenuates isoproterenol-induced cardiac hypertrophy associated with the hdac2 and akt/ gsk-3β signaling pathway. Chem Biol Interact. 2019;307:21–8.
27. Wang H, Mizuno K, Takahashi N, Kobayashi E, Shirakawa J, Terauchi Y, et al. Melanophilin accelerates insulin granule fusion without predocking to the plasma membrane. Diabetes. 2020;69:2655–66.
28. Wang H, Yuan Y-C, Chang C, Izumi T, Wang H-H, Yang J-K. The signaling protein giv/girdin mediates the nephrin-dependent insulin secretion of pancreatic islet β cells in response to high glucose. J Biol Chem. 2023;299.
29. Dunn KW, Kamocka MM, McDonald JH. A practical guide to evaluating colocalization in biological microscopy. Am J Physiology-Cell Physiol. 2011;300:C723–42.
30. Corradi D, Callegari S, Maestri R, Ferrara D, Mangieri D, Alinovi R, et al. Differential structural remodeling of the left-atrial posterior wall in patients affected by mitral regurgitation with or without persistent atrial fibrillation: a morphological and molecular study. J Cardiovasc Electrophys. 2012;23:271–9.
31. Corradi D. Atrial fibrillation from the pathologist's perspective. Cardiovasc Pathology: Official J Soc Cardiovasc Pathol. 2014;23:71–84.
32. Ai Z, Fischer A, Spray DC, Brown AM, Fishman GI. Wnt-1 regulation of connexin43 in cardiac myocytes. J Clin Invest. 2000;105:161–71.
33. Hagendorff A, Schumacher B, Kirchhoff S, Lüderitz B, Willecke K. Conduction disturbances and increased atrial vulnerability in connexin40-deficient mice analyzed by transesophageal stimulation. Circulation. 1999;99:1508–15.
34. Tribulova N, Egan Benova T, Szeiffova Bacova B, Viczenczova C, Barancik M. New aspects of pathogenesis of atrial fibrillation: remodelling of intercalated discs. J Physiol Pharmacol. 2015;66:625–34.
35. Kim B, Song TY, Jung KY, Kim SG, Cho EJ. Direct interaction of menin leads to ubiquitin-proteasomal degradation of β-catenin. Biochem Biophys Res Commun. 2017;492:128–34.
36. Chen C, Zhu D, Zhang H, Han C, Xue G, Zhu T, et al. Yap-dependent ubiquitination and degradation of β-catenin mediates inhibition of wnt signalling induced by physalin f in colorectal cancer. Cell Death Dis. 2018;9:591.
37. Li VS, Ng SS, Boersema PJ, Low TY, Karthaus WR, Gerlach JP, et al. Wnt signaling through inhibition of β-catenin degradation in an intact axin1 complex. Cell. 2012;149:1245–56.
38. Lai CH, Pandey S, Day CH, Ho TJ, Chen RJ, Chang RL et al. B-catenin/lef1/igf-iir signaling axis galvanizes the angiotensin-ii- induced cardiac hypertrophy. Int J Mol Sci. 2019;20.
39. van Roy F, Berx G. The cell-cell adhesion molecule e-cadherin. Cell Mol Life Sci. 2008;65:3756–88.
40. Valenta T, Hausmann G, Basler K. The many faces and functions of β-catenin. Embo j. 2012;31:2714–36.
41. Bian J, Dannappel M, Wan C, Firestein R. Transcriptional regulation of wnt/β-catenin pathway in colorectal cancer. Cells. 2020;9.
42. Kanczuga-Koda L, Wincewicz A, Fudala A, Abrycki T, Famulski W, Baltaziak M, et al. E-cadherin and β-catenin adhesion proteins correlate positively with connexins in colorectal cancer. Oncol Lett. 2014;7:1863–70.
43. Li H, Liu S, Jin R, Xu H, Li Y, Chen Y, et al. Pyrvinium pamoate regulates mgmt expression through suppressing the wnt/β-catenin signaling pathway to enhance the glioblastoma sensitivity to temozolomide. Cell Death Discovery. 2021;7:288.

44. Fukui A, Ikebe-Ebata Y, Kondo H, Saito S, Aoki K, Fukunaga N, et al. Hyperleptinemia exacerbates high-fat diet-mediated atrial fibrosis and fibrillation. J Cardiovasc Electrophys. 2017;28:702–10.
45. Deli MA, Saraswati S, Alfaro MP, Thorne CA, Atkinson J, Lee E et al. Pyrvinium, a potent small molecule wnt inhibitor, promotes wound repair and post-mi cardiac remodeling. PLoS ONE. 2010;5.
46. Lv X, Li J, Hu Y, Wang S, Yang C, Li C, et al. Overexpression of mir-27b-3p targeting wnt3a regulates the signaling pathway of wnt/β-catenin and attenuates atrial fibrosis in rats with atrial fibrillation. Oxid Med Cell Longev. 2019;2019:5703764.
47. Yang H, Wu C, Xiao Y, Zhou S. Connexin and fibrosis related micrornas in complex fractionated atrial electrograms. Archives Med Science: AMS. 2015;11:679–82.
48. Gros DB, Jongsma HJ. Connexins in mammalian heart function. BioEssays: News Reviews Mol Cell Dev Biology. 1996;18:719–30.
49. Giepmans BN. Gap junctions and connexin-interacting proteins. Cardiovascular Res. 2004;62:233–45.
50. Burstein B, Comtois P, Michael G, Nishida K, Villeneuve L, Yeh YH, et al. Changes in connexin expression and the atrial fibrillation substrate in congestive heart failure. Circul Res. 2009;105:1213–22.
51. Liu X, Shi HF, Tan HW, Wang XH, Zhou L, Gu JN. Decreased connexin 43 and increased fibrosis in atrial regions susceptible to complex fractionated atrial electrograms. Cardiology. 2009;114:22–9.
52. Meraviglia V, Azzimato V, Colussi C, Florio MC, Binda A, Panariti A, et al. Acetylation mediates cx43 reduction caused by electrical stimulation. J Mol Cell Cardiol. 2015;87:54–64.
53. Pfannmüller B, Boldt A, Reutemann A, Duerrschmidt N, Krabbes-Graube S, Mohr FW, et al. Gender-specific remodeling in atrial fibrillation? Thorac Cardiovasc Surg. 2013;61:66–73.
54. Ryu K, Li L, Khrestian CM, Matsumoto N, Sahadevan J, Ruehr ML, et al. Effects of sterile pericarditis on connexins 40 and 43 in the atria: correlation with abnormal conduction and atrial arrhythmias. Am J Physiol Heart Circ Physiol. 2007;293:H1231–1241.
55. Tuomi JM, Tyml K, Jones DL. Atrial tachycardia/fibrillation in the connexin 43 g60s mutant (oculodentodigital dysplasia) mouse. Am J Physiol Heart Circ Physiol. 2011;300:H1402–1411.
56. Nakashima T, Ohkusa T, Okamoto Y, Yoshida M, Lee J-K, Mizukami Y, et al. Rapid electrical stimulation causes alterations in cardiac intercellular junction proteins of cardiomyocytes. Am J Physiol Heart Circ Physiol. 2014;306:H1324–33.
57. Qu J, Zhou J, Yi XP, Dong B, Zheng H, Miller LM, et al. Cardiac-specific haploinsufficiency of beta-catenin attenuates cardiac hypertrophy but enhances fetal gene expression in response to aortic constriction. J Mol Cell Cardiol. 2007;43:319–26.
58. Haq S, Michael A, Andreucci M, Bhattacharya K, Dotto P, Walters B, et al. Stabilization of beta-catenin by a wnt-independent mechanism regulates cardiomyocyte growth. Proc Natl Acad Sci USA. 2003;100:4610–5.
59. Orsulic S, Huber O, Aberle H, Arnold S, Kemler R. E-cadherin binding prevents beta-catenin nuclear localization and beta-catenin/lef-1-mediated transactivation. J Cell Sci. 1999;112(Pt 8):1237–45.

Publisher's Note